Brain Struct Funct (2016) 221:1465–1480
DOI 10.1007/s00429-014-0984-5

ORIGINAL ARTICLE

Congenital blindness affects diencephalic but not mesencephalic structures in the human brain

Luca Cecchetti · Emiliano Ricciardi · Giacomo Handjaras · Ron Kupers · Maurice Ptito · Pietro Pietrini

Received: 11 July 2014 / Accepted: 28 December 2014 / Published online: 6 January 2015

Abstract While there is ample evidence that the structure and function of visual cortical areas are affected by early visual deprivation, little is known of how early blindness modifies subcortical relay and association thalamic nuclei, as well as mesencephalic structures. Therefore, in the present multicenter study, we used MRI to measure volume of the superior and inferior colliculi, as well as of the thalamic nuclei relaying sensory and motor information to the neocortex, parcellated according to atlas-based thalamo-cortical connections, in 29 individuals with congenital blindness of peripheral origin (17 M, age 35.7 ± 14.3 years) and 29 sighted subjects (17 M, age 31.9 ± 9.0). Blind participants showed an overall volume reduction in the left ($p = 0.008$) and right ($p = 0.007$) thalami, as compared to the sighted individuals. Specifically, the lateral geniculate (i.e., primary visual thalamic relay nucleus) was 40 % reduced (left: $p = 4 \times 10^{-6}$, right: $p < 1 \times 10^{-6}$), consistent with findings from animal studies. In addition, associated thalamic nuclei that project to temporal (left: $p = 0.005$, right: $p = 0.005$), prefrontal (left: $p = 0.010$, right: $p = 0.014$), occipital (left: $p = 0.005$, right: $p = 0.023$), and right premotor ($p = 0.024$) cortical regions were also significantly reduced in the congenitally blind group. Conversely, volumes of the relay nuclei directly involved in auditory, motor, and somatosensory processing were not affected by visual deprivation. In contrast, no difference in volume was observed in either the superior or the inferior colliculus between the two groups. Our findings indicate that visual loss since birth leads to selective volumetric changes within diencephalic, but not mesencephalic, structures. Both changes in reciprocal cortico-thalamic connections or modifications in the intrinsic connectivity between relay and association nuclei of the thalamus may contribute to explain these alterations in thalamic volumes. Sparing of the superior colliculi is in line with their composite, multisensory projections, and with their not exclusive visual nature.

Keywords Thalamus · Superior colliculus · Lateral geniculate nucleus · Congenital blindness · Morphometry

Electronic supplementary material The online version of this article (doi:10.1007/s00429-014-0984-5) contains supplementary material, which is available to authorized users.

L. Cecchetti · E. Ricciardi (✉) · G. Handjaras · P. Pietrini
Laboratory of Clinical Biochemistry and Molecular Biology, Department of Surgery, Medical, Molecular Pathology, and Critical Area, University of Pisa, Pisa, Italy
e-mail: emiliano.ricciardi@bioclinica.unipi.it

L. Cecchetti · G. Handjaras · P. Pietrini
Clinical Psychology Branch, Pisa University Hospital, Pisa, Italy

R. Kupers · M. Ptito
BRAINlab, Department of Neuroscience and Pharmacology, Panum Institute, University of Copenhagen, Copenhagen, Denmark

M. Ptito
Harland Sanders Chair, School of Optometry, University of Montreal, Montreal, Canada

M. Ptito
Laboratory of Neuropsychiatry, Psychiatric Centre Copenhagen and Department of Neuroscience and Pharmacology, University of Copenhagen, Copenhagen, Denmark

Introduction

Among sensory modalities, vision has a key role in defining how humans acquire knowledge and interact with the surrounding world. From more 'perceptual' tasks, such

as spatial localization, shape, size, and depth discrimination, to more 'cognitive' tasks, including object recognition or social interaction, human behavior, and that of non-human primates, is highly influenced by the strong reliance on vision (Pavani et al. 2000; Ehrsson 2007). In addition, the importance of the visual modality is reflected not only by the number of subcortical structures involved but also by the large proportion of the neocortical surface dedicated to the processing of visual stimuli (Felleman and Van Essen 1991). Unsurprisingly, loss of vision leads to 'plastic' adaptive modifications in the structural and functional architecture of the 'visual' brain, especially when blindness onset occurs at birth or at an early stage of life (Berardi et al. 2000; Karlen et al. 2006). Indeed, several studies in both early and late blind individuals reported atrophy in gray and white matter structures of the 'visual' pathway, affecting the optic nerves, chiasm and radiations, lateral geniculate nucleus, pulvinar, splenium of corpus callosum, as well as striate and extrastriate visual cortical areas (Noppeney et al. 2005; Shimony et al. 2006; Pan et al. 2007; Ptito et al. 2008; Shu et al. 2009; Lepore et al. 2010; Tomaiuolo et al. 2014; Wang et al. 2014). In contrast, other studies demonstrated that early blind individuals retain a normally developed stria of Gennari (Trampel et al. 2011). Other alterations include an increased cortical thickness in the occipital pole (Bridge et al. 2009; Jiang et al. 2009; Park et al. 2009) and modified cortico-cortical connectivity patterns (Klinge et al. 2010; Collignon et al. 2013; Ioannides et al. 2013). Furthermore, blind individuals activate 'visual' cortical areas when performing a variety of non-visual perceptual and cognitive tasks (Pietrini et al. 2004; Ptito and Desgent 2006; Noppeney 2007; Bonino et al. 2008; Cattaneo et al. 2008; Ricciardi et al. 2009; Merabet and Pascual-Leone 2010; Kupers et al. 2011; Kupers and Ptito 2014) and this recruitment is due to two distinct brain processes. First, a large extent of the brain structural and functional cortical architecture develops also in the absence of any visual experience and is able to process information independently from the sensory modality through which it has been acquired—a property named *supramodality*—both in sighted and sensory-deprived individuals (Pietrini et al. 2004; Ricciardi et al. 2007, 2009, 2013, 2014; Ricciardi and Pietrini 2011). Second, visual experience does shape cortical brain development. Therefore, loss of sight, especially at birth or in the early phases of life, and the consequent recruitment of the occipital cortex by alternate sensory/cognitive functions, may be specifically related to a widespread cross-modal plastic rearrangement of connectivity patterns that extends well beyond (the usual limits of) vision-related cortical structures (Ricciardi and Pietrini 2011; Kupers and Ptito 2014; Qin et al. 2014; Ricciardi et al. 2014).

Several findings challenged the hypothesis that structural and functional brain modifications in early blindness predominantly involve the neocortex (Bavelier and Neville 2002; Bridge et al. 2009), and demonstrated rather that congenital blindness also affects certain subcortical structures, not directly involved in visual perception. For instance, the volume of the posterior portion of the right hippocampus is reduced in congenital blindness (Chebat et al. 2007, Lepore et al. 2009), while its anterior portion is enlarged (Fortin et al. 2008). Further subcortical modifications occur in the putamen (Bridge et al. 2009) and the cortico-spinal tract of blind subjects (Yu et al. 2007).

During development, subcortical regions are shaped by sensory inputs (Sur et al. 1988), and their cortical projections have a relevant role determining the functional architecture of the whole-brain (Frost et al. 2000; Sharma et al. 2000; Von Melchner et al. 2000). In the absence of visual input from birth, the development of subcortical structures mainly involved in non-visual processing can take an alternative trajectory. For example, bilateral enucleation in short-tailed opossums alters the overall volume of subcortical regions like the thalamus, the midbrain, and the rhombencephalon (Karlen and Krubitzer 2009; Desgent and Ptito 2012). Among these structures, the thalamus plays an important part in the sensory processing and integration, given its key position in establishing input–output connections between multiple sensory and motor cortical areas (Cappe et al. 2009). In conditions of early visual deprivation, reorganization of the interconnections between thalamic nuclei and the whole thalamo-cortical projection network can occur (Sur et al. 1988; Ghazanfar and Schroeder 2006), leading to functional and morphometric alterations of specific thalamic subregions in the adult. A vast literature in animal models of visual deprivation has described the alterations that occur in the architecture of the metathalamus, which comprises the lateral and medial geniculate bodies (Sakakura and Iwama 1967; Headon and Powell 1973; Cullen and Kaiserman-Abramof 1976; Desgent and Ptito 2012). In sharp contrast to the abundance of animal studies, only a few studies on visual deprivation in humans with congenital anophthalmia (Bridge et al. 2009) or acquired glaucoma (Gupta et al. 2009; Chen et al. 2013; Lee et al. 2014) have reported structural changes in the metathalamic nuclei, but none of them examined potential modifications in thalamic subregions.

Another important structure involved in visual processing is the superior colliculus, a phylogenetically ancient laminated structure (Hilbig et al. 1999; White and Munoz 2011) that, together with the inferior colliculus, constitutes the mesencephalic tectum. In human and in non-human primates, similar to other mammals, the most superficial strata of the superior colliculus receive direct retinal inputs

(Tiao and Blakemore 1976; Wallace et al. 1996; May 2006) and project to striate and extrastriate visual areas (White and Munoz 2011). Therefore, the retinotectal system is considered to be part of the visual pathway. Although the superior colliculus is retinotopically organized (DuBois and Cohen 2000; Sylvester et al. 2007; Limbrick-Oldfield et al. 2012), it also contributes to visual perception without awareness (Leh et al. 2006, 2010) and to spatial attention (Schneider and Kastner 2009; Katyal et al. 2010); its deeper layers are involved in saccades and gaze control (Krebs et al. 2010), as well as in multisensory integration (Sparks and Hartwich-Young 1989; Wallace and Stein 1994; Burnett et al. 2004).

To our knowledge, only a few studies investigated the structure of the human mesencephalic tectum by means of in vivo techniques, and particularly focused on the changes induced by neoplastic (Sherman et al. 1987) and neurodegenerative diseases (Masucci et al. 1995; Warmuth-Metz et al. 2001). While some animal studies reported dramatic volumetric and cytoarchitectonic modifications in the superior colliculus of enucleated (Lund and Lund 1971; Rhoades 1980; Smith and Bedi 1997) and genetically blind rodents (Crish et al. 2006), a study on unilateral cortical blindness following hemispherectomy in the monkey showed that the superior colliculus retained its functionality, despite a notable volume reduction (Theoret et al. 2001). Most importantly, to date, there are no studies that have investigated the effects of visual deprivation since birth on the human superior colliculus.

Here, using a multicenter sample of congenitally blind subjects and in vivo MR imaging, we assessed whether lack of sight since birth causes volumetric and morphometric changes within the thalamic nuclei or the mesencephalic tectum. In particular, we defined the specific volumetric changes of thalamic subregions relaying sensory and motor information to the neocortex, parcellated according to atlas-based thalamo-cortical connections. Thalamic nuclei projecting to the temporal, prefrontal, and occipital cortical regions were altered in congenitally blind subjects, as compared to a matched sighted cohort. On the other hand, thalamic nuclei projecting to posterior parietal, auditory, somatosensory, and motor cortices, as well as the superior and inferior colliculi were not affected by the absence of sight.

Materials and methods

Subjects

Twenty-nine congenitally blind (CB, 17 M, age 35.7 ± 14.3 years) and 29 sighted control subjects (SC, 17 M, age 31.9 ± 9.0 years) recruited at three different research centers (Laboratory of Clinical Biochemistry and Molecular Biology in Pisa, Italy; BRAINlab in Copenhagen, Denmark; School of Optometry in Montreal, Canada) participated in the study. Specifically, 11 CB and 11 SC belonged to the Italian, 10 CB and 10 SC to the Danish, and 8 CB and 8 SC to the Canadian sample. There were no age differences between sighted and blind subjects (t (56) = 1.20, p = 0.24). Causes of blindness are summarized in Table 1. All subjects were blind since birth.

All participants underwent a medical examination in order to exclude history or presence of any medical, neurological, and/or psychiatric disorder, other than blindness in the CB, that could affect brain morphology or function and gave their written informed consent after the study procedures and the risks involved had been explained. The Institutional Ethics Committee of each respective research center approved the protocol and the study was conducted in accordance to the Declaration of Helsinki.

MR acquisition

Italian participants were scanned using a 1.5 T GE Signa Excite magnet; for each participant, a three-dimensional fast spoiled gradient recall (3D-FSPGR) T1 was collected as follows: repetition time (TR) = 2,270 ms, echo time (TE) = 3.6 ms, flip angle (FA) = 10°, field of view (FOV) = 240 × 240 mm, acquisition matrix = 512 × 512, in-plane resolution = 0.47 × 0.47 mm, slice thickness = 1 mm, 150 axial slices. The obtained images were then resampled to a 1 × 1 × 1 mm resolution, in order to match the voxel dimensions of the other two samples involved in the study. Danish participants were scanned using a 3 T Siemens Trio scanner with the following parameters: 3D-MPRAGE T1, TR = 1,540 ms, TE = 3.9 ms, FA = 30°, FOV = 256 × 256 mm, acquisition matrix = 256 × 256, in-plane resolution = 1 × 1 mm, slice thickness = 1 mm, 192 sagittal slices. For the Canadian volunteers, structural images of the brain were collected on a 1.5 T Siemens Magnetom Avanto scanner (3D-MPRAGE T1, TR = 2,240 ms, TE = 9.2 ms, FA = 10°, FOV = 256 × 256 mm, acquisition matrix = 256 × 256, in-plane resolution = 1 × 1 mm, slice thickness = 1 mm, 160 sagittal slices).

Data analysis

Data analysis was carried out using ROBEX v1.2 (http://www.nitrc.org/projects/robex), SPM v8.0 (http://www.fil.ion.ucl.ac.uk/spm/), FSL tools -FMRIB Software Library v5.0 (Smith et al. 2004; Jenkinson et al. 2012; http://fsl.fmrib.ox.ac.uk/fsl/fslwiki/FSL), Caret v5.65 (Van Essen et al. 2001; http://www.nitrc.org/projects/caret/), 3dViewer

Table 1 Demographic and anamnestic data for the CB participants

Subjects				Characteristics of blindness	
ID	Gender	Age	Hand	Cause	Onset
CB01	F	49	R	Retinopathy of prematurity	Birth
CB02	M	41	R	Retinitis pigmentosa	Birth
CB03	M	39	R	Retinal detachment	Birth
CB04	M	58	R	Congenital cataract	Birth
CB05	M	38	R	Retinopathy of prematurity	Birth
CB06	F	31	R	Glaucoma, aniridia	Birth
CB07	M	20	R	Leber's amaurosis	Birth
CB08	M	23	R	Congenital cataract	Birth
CB09	M	27	R	Fibroplasia	Birth
CB10	F	27	R	Optic nerve atrophy	Birth
CB11	F	42	R	Retinopathy of prematurity	Birth
CB12	M	60	R	Congenital glaucoma	Birth
CB13	F	31	R	Microphthalmia + congenital cataract	Birth
CB14	F	23	R	Optic nerve atrophy	Birth
CB15	M	35	R	Retinopathy of prematurity	Birth
CB16	M	57	R	Congenital cataract	Birth
CB17	M	58	R	Congenital glaucoma	Birth
CB18	F	19	R	Congenital glaucoma	Birth
CB19	F	63	R	Congenital glaucoma	Birth
CB20	F	26	R	Retinopathy of prematurity	Birth
CB21	M	56	R	Retinopathy of prematurity	Birth
CB22	F	21	R	Retinopathy of prematurity	Birth
CB23	M	21	R	Retinopathy of prematurity	Birth
CB24	F	41	R	Retinopathy of prematurity	Birth
CB25	M	19	R	Retinopathy of prematurity	Birth
CB26	M	23	L	Retinopathy of prematurity	Birth
CB27	F	27	R	Retinopathy of prematurity	Birth
CB28	M	35	R	Unknown	Birth
CB29	M	23	R	Glaucoma	Birth

plugin for ImageJ (Schmid et al. 2010; http://3dviewer.neurofly.de/), MathWorks MATLAB Release 2012a (http://www.mathworks.com/products/matlab/), and IBM SPSS v21.0.0 (http://www-01.ibm.com/software/uk/analytics/spss/).

In the common preprocessing for all the further analysis, MRI acquisitions were brain extracted using ROBEX (Iglesias et al. 2011), an automatic algorithm that robustly removes non-brain tissues from T1-weighted scan, so as to ensure the stability/robustness of subsequent critical steps in the analysis pipeline, such as the spatial transformation in the standard space and tissue type segmentation (Iglesias et al. 2011).

Global and local volume estimation of the thalamus

The open source software package FSL v5.0 was adopted as a tool to accurately estimate the effects of congenital blindness on visual and non-visual thalamic nuclei volumes. Specifically, brain-extracted MR images were segmented into white matter (WM), gray matter (GM), and cerebrospinal fluid (CSF) and corrected for radiofrequency pulse inhomogeneity, using the method proposed by Zhang and collaborators and implemented in FSL-FAST v4.1 (Zhang et al. 2001). The unbiased T1-weighted images were then spatially transformed to match the 1 mm^3 MNI152 brain template (Fonov et al. 2011), using FSL-FLIRT (Jenkinson et al. 2002). This procedure included a two-step affine transformation, to minimize the alignment error of subcortical structures arising from spatial registration (Patenaude et al. 2011). First, a whole-brain linear transformation with 12 degrees of freedom was estimated for initial resampling to standard space. Next, a transformation was computed using a mask solely of the subcortical structures (bilateral thalamus, hippocampus, amygdala, lentiform and caudate nuclei), and then applied to the entire brain.

Additionally, in order to characterize the shape and volume of the thalamus, a Bayesian shape and appearance segmentation model (Patenaude et al. 2011) was applied to the preprocessed images (FSL-FIRST v5.0.0). In brief, to this end a three-dimensional mesh was iteratively deformed to match the shape of the thalamus, while the voxel intensity was used to judge the goodness of fit. This novel and automatic procedure takes advantage of a training set comprising 336 manually labeled T1-weighted images and of the typical fixed topology of subcortical structures in order to define precisely the region of interest (ROI) corresponding to the thalamus. Since the three-dimensional meshes have a fixed number of vertices across subjects, FSL-FIRST estimates group differences not only for the overall volume of the ROI, but also for shape, corresponding respectively to indices of the global and local atrophy/hypertrophy. This latter analysis entails using a univariate test that estimates the mean distance of each vertex between groups (vertex analysis).

Individual thalamic ROIs generated by FSL-FIRST were carefully inspected to exclude the possibility of misclassification of thalamic voxels adjacent to the borders, although no manual correction proved to be necessary. Next, overall volumes of the left and right thalamus were measured for each subject (FSLSTATS) and imported in SPSS to investigate the expected differences in global volume between CB and SC. This hypothesis was tested ($p < 0.05$) through a general linear model (GLM) including group, gender, and scanner site in addition to age and overall brain volume as covariates.

To characterize the exact anatomical location for morphological changes of the thalamus due to congenital blindness, we performed a test on the coordinates of each vertex. A rigid alignment (global rotation and translation) was applied to the individual thalamic meshes, with the purpose of minimizing the sum of square error distance from the average thalamus shape. This procedure ensures the removal of error due to differences in pose of different subjects, while preserving the characteristics of the individual MRI acquisition. Just as for the overall thalamic volume analysis, group, age, gender, MRI scanner location, and total brain volume were included as factors in the GLM. A non-parametric permutation test with 10,000 iterations (Nichols and Holmes 2002) was applied to identify vertices showing significant ($p < 0.05$) displacements between CB and SC, using the threshold-free cluster enhancement (TFCE) method to correct for multiple comparisons (Smith and Nichols 2009).

Finally, to illustrate better regions of local alteration in the CB versus SC contrast, vertex analysis results were overlapped with the Oxford Thalamic Connectivity Probability Atlas (Behrens et al. 2003; Johansen-Berg et al. 2005). This atlas, which is included in the FSL 5.0 Software Library, provides a parcellation of the human thalamus to seven subregions based on thalamo-cortical connectivity, as distinguished in diffusion-weighted acquisitions in conjunction with probabilistic tractography analysis. Consequently, the anatomical locations demonstrating differences between groups were ultimately classified according to the cortical regions normally targeted by their projections: prefrontal, premotor, primary motor, somatosensory, posterior parietal, occipital, and temporal cortices—for a precise definition of the boundaries of cortical regions please refer to Behrens et al., (2003). Thalamic nuclei equivalent to the tractography-defined subregions of the Oxford Thalamic Connectivity Probability Atlas are summarized in Table 2, as proposed by Behrens et al. (2003). To summarize the results of the vertex-wise analysis and improve the readability of their relationship with the connectivity atlas, we built a flattened version of the thalamus. In brief, the 3-dimensional mesh was imported into Matlab and processed using the dpv2map tool, part of the Areal package (Winkler et al. 2012; http://brainder.org/download/areal/). The obtained surface comprised both atlas values and vertex-wise statistics for group comparisons and was then imported into Blender (http://www.blender.org/), cut in the dorsal part along the rostro-caudal axis of the thalamus and flattened, thereby correcting for geometrical distortions.

Therefore, for each of the Oxford Thalamic Connectivity subregions (projected onto the study-specific thalamus template as depicted in Fig. 1), we extracted three 'atrophy scores' for the CB versus SC group comparison: the average T value, the maximum T value, and the proportion of statistically significant vertices. Then, we calculated the Z values across subregions for each score and the specific portions of the thalamus were sorted accordingly from the most atrophic to the most preserved. Thus, the subregions were given a rank for each 'atrophy score' and subsequently we calculated a composite index based on the median rank of the three scores (see histograms in Fig. 1). This may be considered a vertex analysis-based qualitative measure of how congenital loss of sight specifically affects thalamic subregions.

Moreover, to quantify local volume differences within thalamic subregions, we created a 'study-specific thalamus template' by pooling the segmented structures from sighted and blind subjects. Within this 'averaged' thalamus, we estimated the volume of each subregion as the total voxel count weighted by (that is, multiplied by) the Oxford Thalamic Connectivity Probability Atlas values. Subsequently, at a single subject level, a displacement value (i.e., the output of the vertex analysis) was derived for each voxel as the geometric distance between the actual edge of each subject's thalamus and the edge of the *study-specific template*. In addition, for each subject, the grand total of

Table 2 Cortical projections of thalamic nuclei, in accordance to Behrens et al. (2003)

Thalamic nuclei	Projecting to
Lateral posterior (LP); ventral posterolateral (VPL); ventral posteromedial (VPM)	Somatosensory cortex (SSC)
Anterior pulvinar	Posterior parietal cortex (PPC)
Inferior pulvinar; intralaminar	Occipital cortex (OC)
Medial pulvinar; inferior pulvinar; mediodorsal (MD); anterior complex (AC)	Temporal cortex (TC)
Mediodorsal (MD); ventral anterior (VA); anteromedial (AM); anterodorsal (AD)	Prefrontal cortex (PFC)
Anterior part of the ventral lateral (VLa); posterior part of the ventral anterior (VAp)	Premotor cortex (PMC)
Posterior part of the ventral lateral (VLp)	Primary motor cortex (MC)

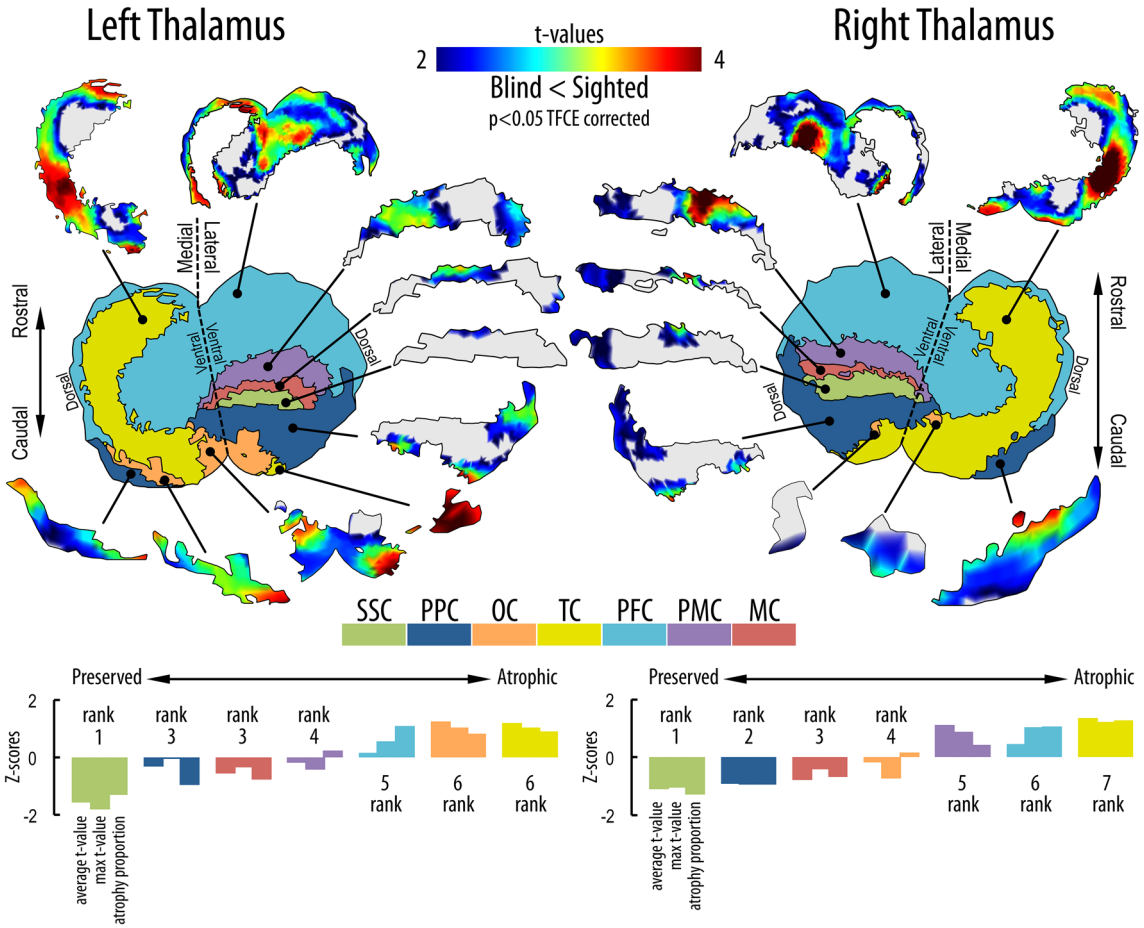

Fig. 1 Vertex-wise analysis in congenitally blind as compared to sighted control subjects. The flattened version of the left and right study-specific thalamus template is shown in the *upper* part of the *panel* and subregions of the Oxford Thalamic Connectivity Probability atlas are projected onto the surface. Vertices projecting to prefrontal (PFC) cortical areas are depicted in *cyan*, premotor cortex (PMC) in *purple*, motor cortex (MC) in *red*, somatosensory cortex (SSC) in *green*, posterior parietal cortex (PPC) in *dark-blue*, temporal cortex (TC) in *yellow*, and occipital cortex (OC) in *orange*. Each subregion is also individually represented to improve the readability of vertex-wise statistics (*T* values for group comparison). In the *lower* part of the *panel*, the *histogram* represents the *Z* scores across subregions for the average *T* value, the maximum *T* value and the atrophy proportion of vertices. Thalamic regions are sorted according to the median rank of the three 'atrophy scores', from the most preserved to the most atrophic. As shown, congenital loss of sight affects the thalamic subregions to different extents. Interestingly, none of the thalamic areas was significantly larger in blind participants

voxel displacements was weighted by connectivity values and was added to the volume of each specific subregion of the thalamic template.

The use of weighted (i.e., non-binary) ROIs takes into account the variability of the region across subjects and allows for an estimation of the atrophy, dealing with the degree of uncertainty on voxel identity. Therefore, volumetric changes between the groups were tested separately for each thalamic ROI by means of a GLM including gender, MRI location, age, and overall brain volume as nuisance variables ($p < 0.05$). Since the Oxford thalamic parcellation comprises seven subregions, a formal correction for multiple comparisons was carried out by means of the false discovery rate (FDR) procedure (Benjamini and Hochberg 1995). In the last step, volume variations were also expressed as percentages (i.e., the average volume difference between groups, divided by the ROI volume of SC and multiplied by 100).

Volumetric analysis of the metathalamus

The metathalamus consists of the lateral and medial geniculate nuclei, respectively LGN and MGN; these are not included in the Oxford Thalamic Connectivity Probability Atlas, and their precise localization and volumetric measurement using T1 acquisitions remains a technical challenge (Gupta et al. 2009; Li et al. 2012). To overcome these problems, we adopted a ROI-based approach that combines an automatic segmentation method (Hernowo et al. 2011) with probabilistic maps registered to the MNI space (Burgel et al. 1999; Rademacher et al. 2002; Eickhoff et al. 2005; Burgel et al. 2006). Metathalamic nuclei are identified by partitioning the T1 brain image into six tissue classes (Hernowo et al. 2011), instead of the common segmentation of the three tissues: gray matter, white matter, and cerebrospinal fluid. The fifth tissue class of this fine grain parcellation, carried out using FSL-FAST v4.1 and based on voxel intensity (Zhang et al. 2001), accounts well for the boundary definition of diencephalic structures of present interest, i.e., the lateral and medial geniculate nuclei. The approach has been successfully used in a report that included normal controls and patients affected by primary open-angle glaucoma (Hernowo et al. 2011). In order to refine the bilateral LGN and MGN segmentation, four spherical ROIs of 10 mm diameter were used as an anatomical prior and were drawn at the center of gravity of the lateral and medial geniculate maps included in the Jülich cytoarchitectonic atlas (Eickhoff et al. 2005).

The maximum volume estimation of each spherical ROI was 524 mm^3, a value that according to previous post-mortem (Zvorykin 1980; Winer 1984; Andrews et al. 1997) and MRI studies (Korsholm et al. 2007; Hernowo et al. 2011; Li et al. 2012; Lee et al. 2014) is adequate to comprise the volume range for left and right lateral and medial geniculate nuclei. Moreover, the 10 mm diameter of the ROI comprises the 4–6 mm LGN height (Gupta et al. 2009; Dai et al. 2011) and accommodates the intersubject variability (Barnes et al. 2010). Once the lateral and medial geniculate nuclei were identified as outlined above, we computed the volume of the metathalamus following the tissue quantification guidelines (http://fsl.fmrib.ox.ac.uk/fsl/fslwiki/FAST). For each subject, the volumes of the LGN and MGN were estimated as the sum of the non-zero probability voxels lying inside the mask, multiplied by (i.e., limited to) the tissue probability map. As for the other ROI analyses, the statistically significant ($p < 0.05$) group differences were estimated using a GLM adding age, gender, MRI site, and overall brain volume as covariates of no interest.

Volumetric analysis of the superior and inferior colliculi

As for the volumetric analysis of the metathalamus, we used a semi-automatic ROI procedure to assess volumetric changes in the superior and inferior colliculi. As a first step, we manually aligned each subject's T1 image to the intercommissural plane (AC–PC line). We then adjusted brightness, contrast, and color scale to facilitate the detection of these mesencephalic structures. Next, the borders of four ROIs (left and right superior and inferior colliculi) were manually drawn on sagittal, coronal, and transverse sections following the definitions of the Duvernoy's atlas of the human brain stem and cerebellum (Naidich et al. 2009). The dorsolateral margins of the superior and inferior colliculi were carefully defined on coronal sections, at the level where they join the respective brachia. We defined the borders of the inferior colliculi on transverse and sagittal sections alongside the medullary lamina, excluding the thin band of the lateral lemniscus. Further, the medial border of the inferior colliculus was traced along the marginal fibers of the periaqueductal gray, while the upper boundary was delineated on a sagittal plane, exactly where the ellipsoidal body of the inferior colliculus joins the lower portion of the superior colliculus (similarly to Kang et al. 2008). The periaqueductal gray was taken to define medial and anterior borders of the superior colliculus, while the quadrigeminal cistern represented its posterior margin.

Once single subjects ROIs were defined, we extracted the absolute volume for each structure as the number of voxels within each mask multiplied by the parenchymal (GM + WM) tissue probability. Finally, we evaluated volumetric differences between blind and sighted participants for each structure (i.e., left and right superior and left and right inferior colliculus; $p < 0.05$) by means of a

GLM, using age, gender, MRI site, and overall brain volume as nuisance variables.

Results

The overall brain parenchymal volume (GM + WM volume) was significantly decreased in congenitally blind subjects (F (1, 46) = 5.334, $p = 0.025$), as compared to sighted individuals. This was confirmed by a whole-brain voxel-based morphometry (VBM) analysis showing patterns of white and gray matter atrophy similar to those available in the literature (see Supplementary Material for details).

Global and local volume estimation of the thalamus

Overall, thalamic volume analysis demonstrated a significant reduction in both the left (F (1, 46) = 7.599, $p = 0.008$) and right thalamus (F (1, 46) = 7.931, $p = 0.007$) of blind participants. Specifically, volumes of the left thalamus (mean ± standard error) were 7,651 ± 102 mm^3 for CB and 8,037 ± 97 mm^3 for SC, whereas corresponding volumes of the right thalamus were 7,462 ± 98 mm^3 and 7,841 ± 93 mm^3, respectively. No gender-related or scanner site-specific effects were found.

Results of the vertex-wise (Fig. 1) and ROI analyses (Fig. 2) demonstrated a specific pattern of atrophy affecting the thalamus in the congenitally blind individuals. Loss of vision significantly altered regions of the left thalamus (Fig. 1 and lower part of Fig. 2b), which are connected with temporal (F(1, 46) = 8.760, FDRc $p = 0.023$), occipital (F (1, 46) = 8.742, FDRc $p = 0.023$) and prefrontal cortical areas (F (1, 46) = 7.217, FDRc $p = 0.035$). These regions had volume reductions of 9.76, 8.51, and 4.54 %, respectively. In addition, the left thalamic nuclei projecting to posterior parietal, somatosensory, premotor, and motor cortices showed no statistically significant atrophy ($p > 0.05$). For the right thalamus, we observed a 9.28 % volume reduction (Fig. 1 and lower part of Fig. 2c) in nuclei projecting to temporal (F (1, 46) = 8.561, FDRc $p = 0.023$), 5.53 % to occipital (F (1, 46) = 5.541, FDRc $p = 0.048$), 4.16 % to premotor (F (1, 46) = 5.430, FDRc $p = 0.048$), and 4.14 % to prefrontal cortex (F (1, 46) = 6.511, FDRc $p = 0.039$). There were no significant volume changes in thalamic nuclei projecting to posterior parietal, motor, and somatosensory cortex.

The heat-map plots located in the upper part of Fig. 2b, c depict the specific 'footprint' of local atrophy in the visually deprived thalami. Here, each thalamic subregion is represented as a two-dimensional frequency distribution of voxels (color), that are characterized by the specificity of their projections (y axis: connectivity scores extracted from the Oxford Thalamic Connectivity Probability Atlas) and by the magnitude of the atrophy in congenitally blind subjects (x axis: T values for CB < SC obtained from the vertex analysis). Indeed, it appears that voxels with higher connectivity values (i.e., with a specific attributable identity) represent the magnitude of local atrophy for the related thalamic subregion. Thus, regions of the thalamus showing the most pronounced volumetric differences between groups (according to the bar charts in the lower part of Fig. 2b, c), have conspicuous clusters of specifically connected voxels that lie well above the statistical threshold (white dashed line: t (56), $p = 0.05$), while thalamic nuclei that are not affected by congenital blindness demonstrate a considerable number of highly connected voxels lying below the threshold. On the other hand, for both impaired and preserved subregions, less specific voxels (that is, those with lower connectivity scores) have a broad range of atrophy scores, which is roughly homogeneous across thalamic nuclei. Therefore, local volume decrements found in thalamic subregions of the CB are not merely driven by differences in the global thalamic volume, but originate from specific patterns of atrophy due to the absence of sight.

Thus, according to our thalamic nuclei classification based on the thalamo-cortical connectivity proposed by Behrens and collaborators (2003), affected regions in the CB group included the inferior and medial pulvinar, the mediodorsal nucleus (MD), the ventral anterior nucleus (VA), and the anterior complex (AC). The ventral lateral (VLp), the anterior pulvinar, the ventral posteromedial (VPM), and the ventral posterolateral (VPL) nuclei did not show significant volumetric changes.

Volumetric analysis of the metathalamus

In sighted controls, the average volumes (mean ± standard error) for the left and right LGN were 135.2 ± 7.2 mm^3 and 133.4 ± 6.4 mm^3, while volumes for the medial geniculate nuclei were 95.7 ± 7.7 mm^3 (left MGN) and 92.4 ± 7.0 mm^3 (right MGN), respectively. Most importantly, a group comparison revealed volume reductions of 38.57 and 47.65 %, respectively for the left (F (1, 46) = 27.180, $p = 4 \times 10^{-6}$) and right (F (1, 46) = 50.426, $p < 1 \times 10^{-6}$) LGN of blind individuals, while volumes of bilateral MGN did not differ between groups (Fig. 3).

Noteworthy, volumetric measurements in our sighted controls were comparable to that reported in previous post-mortem studies, both for the lateral geniculate (Andrews et al. 1997) and the medial geniculate (Winer 1984) nuclei.

Volumetric analysis of the superior and inferior colliculi

Neither the superior nor the inferior colliculi showed any statistically significant difference between the two groups (Fig. 4).

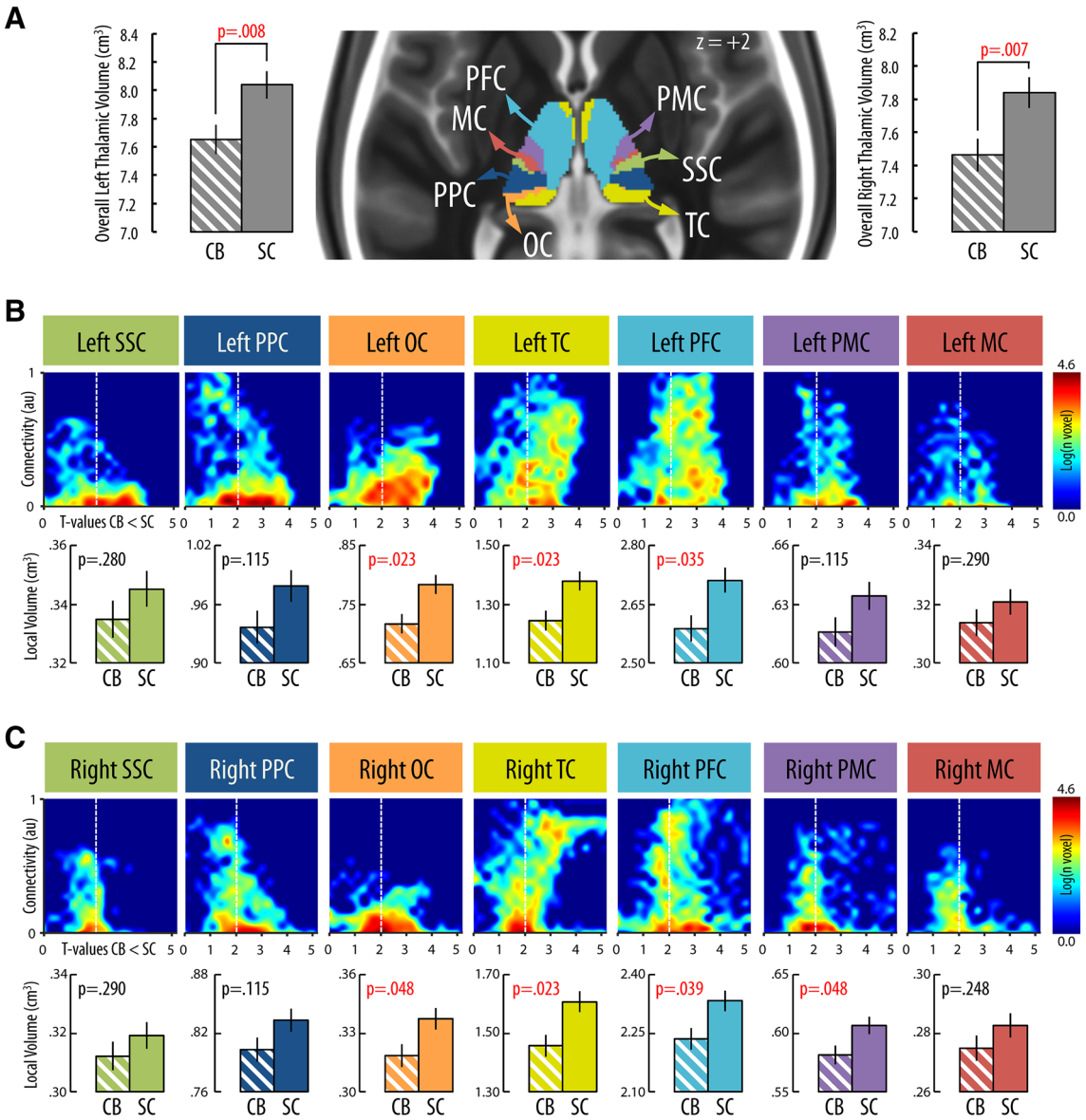

Fig. 2 Results of the ROI analysis. Both the global and local volumes of the thalamus were compared between groups. *Bar charts* in **a** show the statistically significant overall volume reduction in the left and right thalamus of CB. The axial brain slice in **a** represents the '*color-code*' used to define portions of the thalamus according to the Oxford Thalamic Connectivity Probability Atlas (Behrens et al. 2003; Johansen-Berg et al. 2005). The figure also shows local volume loss for the left (**b**) and right (**c**) subregions of the thalamus projecting to SSC (*green*), PPC (*blue*), OC (*orange*), TC (*yellow*) PFC (*cyan*), PMC (*purple*), and MC (*red*). The *bar charts* located in the *lower* part of these *panels* reveal thalamic subregions showing a statistically significant volume reduction due to congenital blindness. In agreement with this, the *upper* part of the *panels* shows that regions affected by lack of vision have a noticeable proportion (*hotter colors*) of highly specific voxels (with higher scores of connectivity), demonstrating larger spatial displacement values between groups (higher T values for CB < SC). The *white dashed line* represents t (56), $p = 0.05$, just for readability purpose

Specifically, the average volumes of the superior colliculus of sighted controls (mean ± standard error) were 180.2 ± 4.9 mm^3 (left) and 169.8 ± 4.4 mm^3 (right), compared to 175.9 ± 5.2 mm^3 (left) and 166.6 ± 4.4 mm^3 (right) for congenitally blind subjects. Volumes of the left and right inferior colliculus were, respectively, 117.7 ± 4.0 mm^3 and 110.6 ± 3.9 mm^3 for SC, and 121.7 ± 4.2 mm^3 and 108.2 ± 4.1 mm^3 for CB.

Discussion

In a multicenter MRI study sample of blind individuals contrasted with a matched sighted control group, we demonstrated that congenital loss of sight leads to an overall thalamic volume reduction. The lateral geniculate nucleus (i.e., the main visual thalamic relay) and the thalamic association nuclei projecting to the temporal

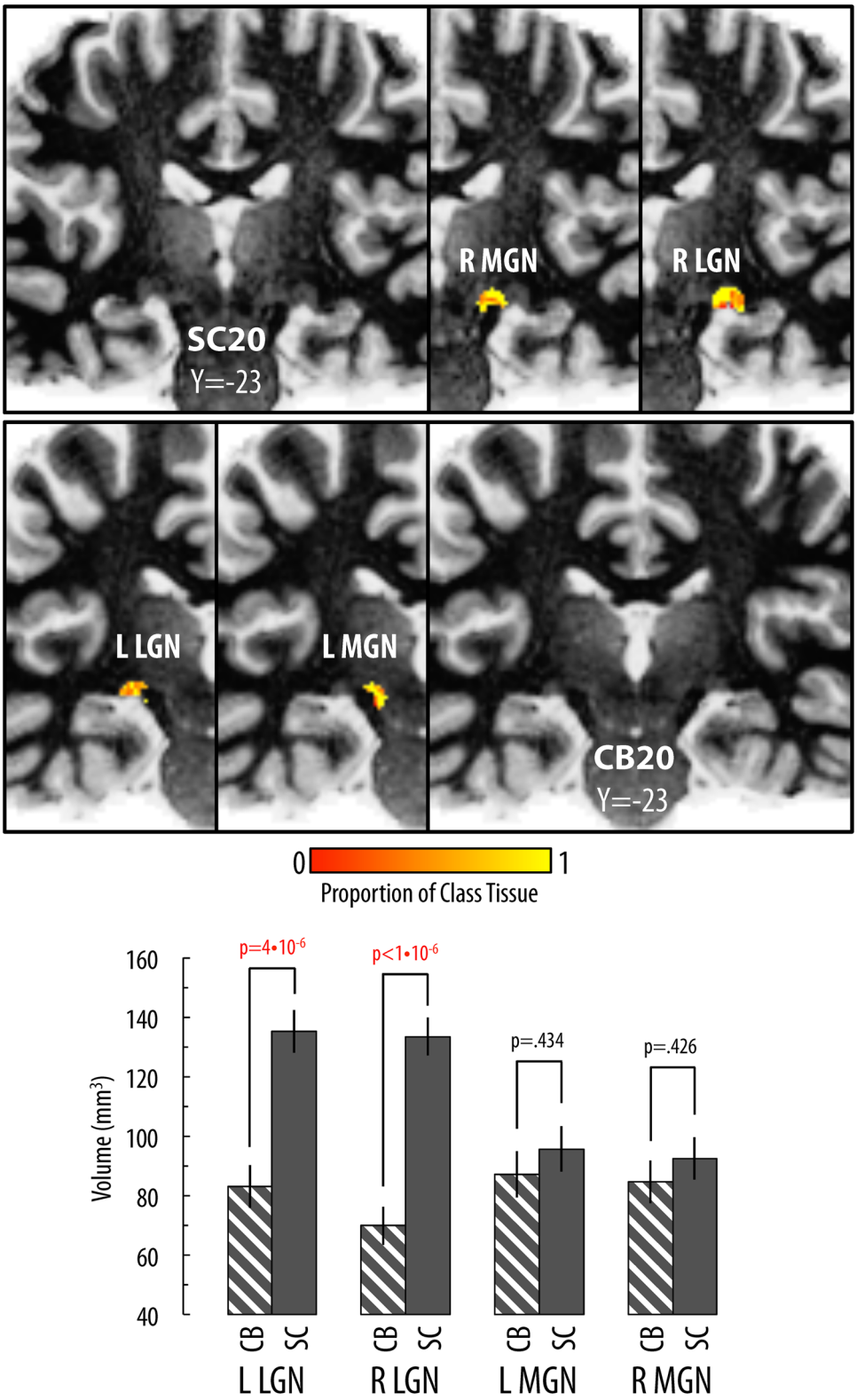

Fig. 3 Results for the volumetric analysis of lateral (LGN) and medial (MGN) geniculate nucleus. The *upper* part of the *panel* depicts the LGN and MGN segmentation in two representative subjects. The *histogram*, located in the *lower* part of the figure, reveals a significant difference ($p < 0.05$) between CB and SC in the bilateral LGN but not in the MGN

(anterior complex, inferior, and medial pulvinar), right premotor (ventral anterior), prefrontal (mediodorsal), and occipital (inferior pulvinar) cortical areas were affected. Interestingly, non-visual (auditory, motor, and somatosensory) relay nuclei, such as the medial geniculate, posterior part of ventral lateral, ventral posteromedial, and ventral

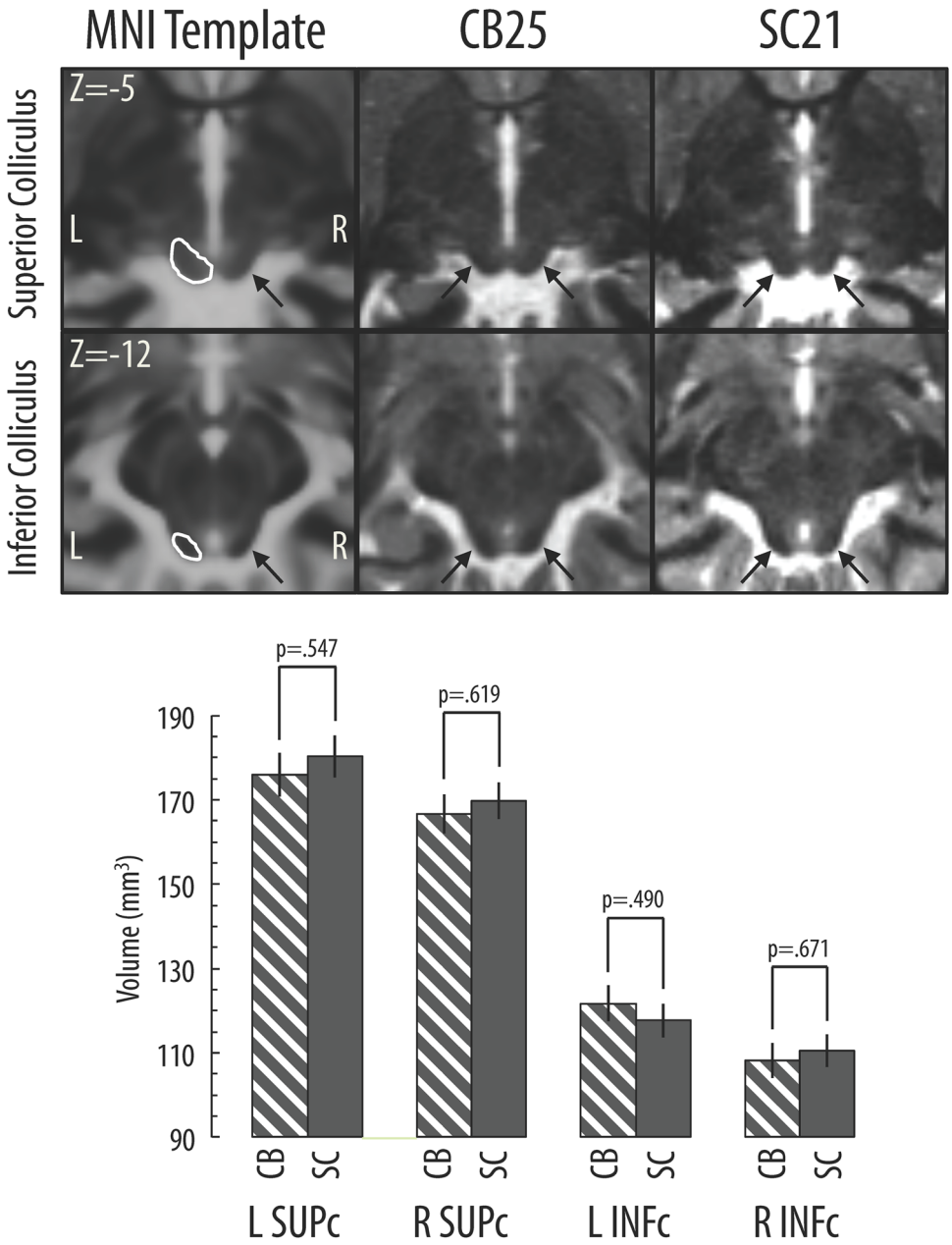

Fig. 4 Volumetric analysis of the superior (SUPc) and inferior (INFc) colliculus. The *upper* part of the *panel* illustrates the delineation of these structures for the MNI template (*white line* and *black arrow*) and for two representative subjects (*black arrows*), CB25 and SC21. No significant differences between CB and SC were found for either the superior or inferior colliculus (*bar chart*, *lower* part)

posterolateral nuclei, were not reduced in volume. Of note, these nuclei did not show volume increases either, which is in contrast with what one might expect as previous studies showed a significant hypertrophy in both the somatosensory (Noppeney et al. 2005) and motor (Yu et al. 2007) pathways of blind subjects. Furthermore, in contrast to what one would expect based on results from animal studies, the superior colliculus in the congenitally blind individuals was preserved, indicating that the atrophy within the subcortical visual pathways is limited to diencephalic structures. The mesencephalic component of the auditory system (i.e., the inferior colliculus) was also within the normal range in congenitally blind subjects, thus suggesting that visual deprivation does not lead to a plasticity-induced compensatory hypertrophy in the subcortical auditory pathway.

The present findings expand the observation of volumetric and metabolic changes found in the neocortex of congenitally blind individuals (see Kupers and Ptito 2011, 2014), by demonstrating that corresponding changes also occur in thalamic nuclei that project to their specific cortical target.

In general, sensory deprivation, especially at an early stage of development, results in a functional reorganization of the brain, which comes to rely more on the remaining sensory inputs. Consequently, cortical and subcortical

visual structures in congenitally blind subjects undergo cross-modal plastic modifications that reshape their anatomical and physiological organization, making them more responsive to non-visual perceptual and cognitive tasks (Pietrini et al. 2004; Noppeney et al. 2005; Ricciardi et al. 2009; Kupers and Ptito 2011, 2014; Tomaiuolo et al. 2014).

The present data demonstrate that local atrophy of the primary visual relay nuclei, and also of the association nuclei in CB individuals, constitutes a specific pattern rather than some non-specific global reduction of the thalamus deprived of its normal visual input. In order to better define the 'footprint' of local volumetric alterations, the changes revealed by the vertex-wise analysis were assigned to still smaller subregions, parcellated according to their thalamo-cortical connections, as defined in the Oxford Atlas (Fig. 2). Notably, although each division of the thalamus comprises both 'aspecific' (those with lower connectivity scores) and highly specific (those with higher cortical connectivity rates) voxels, it is the latter group that determines the local volume reduction in the CB. Hence, thalamic voxels assigned less cortical connectivity have a wider range of "atrophy" scores, homogeneous across thalamic nuclei. Thus, within each thalamic subregion, those clusters with a distinct 'identity' in terms of their normal connectivity were preserved or affected by congenital loss of sight in a manner consistent with their functional role, and the predictability of their cortical projections. Again, this finding supports our hypothesis that subregional volume decrements in CB are not simply a consequence of a decline in the global thalamic volume, but arise from a specific pattern of atrophy due to the congenital absence of sight.

Two distinct mechanisms might be put forward to explain the thalamic volume loss in congenitally blind individuals, namely (1) changes in reciprocal thalamo-cortical connections and (2) changes in the intrinsic connectivity between thalamic relay and association nuclei. We found volume loss in both primary visual and association thalamic nuclei, including the pulvinar and the mediodorsal nuclei. The association nuclei integrate multiple sensory and motor inputs/outputs, and have a pivotal role in regulating the neural activity of associative cortical areas through a complex network of reciprocal connections (Hendelman 2005). We suggest that the lack of visual input triggers a cascade of atrophic or developmental changes, arising first in the LGN, extending to the optic radiations (Ptito et al. 2008; our VBM results), and ultimately further to striate and extrastriate cortices. At the same time, default cortico-cortical connectivity of these normally visual cortical areas with parietal, frontal, and temporal cortical areas are also reduced (Liu et al. 2007), consequently attenuating the feedback connections between parietal, frontal, and temporal cortices with their recipient thalamic nuclei. In this regard, we find it noteworthy that a recent resting state functional connectivity study in the sighted showed that specific thalamic structures exhibit BOLD signal fluctuations in phase with those of their connected cortical regions, underscoring the importance of the cortico-thalamic feedback, and feed-forward projections (Zhang et al. 2008). On the other hand, the results of task-related functional connectivity analyses, mainly involving perceptual tasks, seem to suggest that cross-modal plastic changes in the CB reflect alterations more in cortico-cortical rather than thalamo-cortical connections (Klinge et al. 2010; Collignon et al. 2013; Leo et al. 2012; Kupers and Ptito 2014; but see also Kahn and Krubitzer 2002; Desgent and Ptito 2012).

Alternatively, volume reductions may reflect reshaping of the thalamic maps, a process suggested by Kahn and Krubitzer (2002). According to this view, rewiring of the intrinsic thalamic connections takes place in blindness, leading to a "colonization" of normally visual thalamic nuclei by other nuclei receiving non-visual input. This hypothesis is to a certain extent supported by observations in animal studies. For instance, Heil and colleagues (1991) found that both the visual cortex and the LGN of the blind mole rat receive auditory inputs, while Chabot and collaborators (2007) reported auditory-evoked electrophysiological activity in the LGN of anophthalmic mice. Thus, in the event of the lack of a distinct sensory modality, such as the visual one, the developmental differentiation program may attract other sensory inputs to continue the thalamic maturation (recently reviewed in Ricciardi et al. 2013). Nonetheless, this 'hard-rewiring' hypothesis and the modifications occurring in the cortico-thalamic feedback connections may equally contribute to and reciprocally interact in the reshaping of the thalamus in visually deprived individuals.

Moreover, the mere fact that all retinal inputs are absent since birth should theoretically lead to a degeneration of the dorsal lateral geniculate nucleus (dLGN), as shown in animal models of neonatal enucleation (see Desgent and Ptito 2012, for review). Indeed, in bilaterally enucleated animals, the dLGN is reduced by approximately one half (Heumann and Rabinowicz 1980), although its remaining neurons still project via the optic radiations to the visual cortex. In accordance with that study, and with a previous one conducted on CB humans (Ptito et al. 2008), we now report that early loss of sight leads to a dramatic volume reduction in bilateral LGN and in their striate projections (see Supplementary results). We believe that the remaining LGN stays functional, thanks to the cortico-thalamic inputs it receives from the striate cortex, which has adopted non-visual functions. Indeed, the visual cortex of CB receives two

types of non-visual inputs, arising either through the optic radiations from a dLGN which has been "colonized" by VPL or MGB, and as ectopic projections from mesencephalic structures, such as the inferior colliculus, or through altered cortico-cortical projections back to the dLGN (Ptito and Kupers 2005; Ptito et al. 2005; Kupers et al. 2006; Ioannides et al. 2013).

As far as the superior colliculus is concerned, volumes obtained in the sighted controls using our procedure are in line with those reported in previous studies (Kang et al. 2008; Sabanciogullari et al. 2013) and with those we obtained when using an alternative independent volumetric evaluation on the MNI152 Standard Symmetric Template (see Supplementary Materials). Two factors may explain the lack of volume reduction in the superior colliculus of congenitally blind subjects: (a) a significant proportion of its neurons, located in the deep layers, responds to multisensory inputs (Sparks and Hartwich-Young 1989) and (b) the number of retinotectal projections, that target only the superficial layers of the colliculus (Tiao and Blakemore 1976; Wallace et al. 1996; Katyal et al. 2010), decreases along with the phylogenetical evolution of the geniculostriate system (Schiller 1977; White and Munoz 2011). In conclusion, unlike the lateral geniculate nucleus, the human superior colliculus cannot be regarded as a merely visual structure, and this may explain the lack of significant effects following perinatal visual deprivation.

In summary, using structural MRI in a multicenter study sample of congenitally blind humans, we show that absence of sight reduces by half the volume of the primary visual relay (LGN), with additional significant, though smaller, reductions in non-visual association thalamic nuclei. Importantly, the volumes of the remaining sensory relay nuclei, as well as the superior colliculus, were not affected. We propose a model whereby, because of the absence of vision since birth, the visual relay and association nuclei of the thalamus undergo a massive reorganization of their circuitry through abnormal intra-thalamic connectivity, and the retention of cortico-thalamic projections from the reorganized primary visual cortex (which has assumed non-visual functions), as well as from other cortical regions.

Acknowledgments LC would like to thank Dr. Francesco Tomaiuolo and Dr. Ludwig Barbaro for the helpful comments and suggestions provided. This work was supported by grants from the Italian Ministero dell'Istruzione, dell'Università e della Ricerca (PP, ER, LC, GH), the Lundbeck foundation (RK), the Danish Medical Research Council (MP), and the Harland Sanders Chair in Visual Science (Canada). The authors note professional manuscript proofreading by Inglewood Biomedical Editing.

Conflict of interest None of the authors have any potential conflict of interest related to this manuscript.

References

Andrews TJ, Halpern SD, Purves D (1997) Correlated size variations in human visual cortex, lateral geniculate nucleus, and optic tract. J Neurosci 17:2859–2868

Barnes GR, Li X, Thompson B, Singh KD, Dumoulin SO, Hess RF (2010) Decreased gray matter concentration in the lateral geniculate nuclei in human amblyopes. Invest Ophthalmol Vis Sci 51:1432–1438. doi:10.1167/iovs.09-3931

Bavelier D, Neville HJ (2002) Cross-modal plasticity: where and how? Nat Rev Neurosci 3:443–452. doi:10.1038/nrn848

Behrens TE et al (2003) Non-invasive mapping of connections between human thalamus and cortex using diffusion imaging. Nat Neurosci 6:750–757. doi:10.1038/nn1075

Benjamini Y, Hochberg Y (1995) Controlling the false discovery rate: a practical and powerful approach to multiple testing. J R Stat Soc B 57:289–300

Berardi N, Pizzorusso T, Maffei L (2000) Critical periods during sensory development. Curr Opin Neurobiol 10:138–145

Bonino D et al (2008) Tactile spatial working memory activates the dorsal extrastriate cortical pathway in congenitally blind individuals. Arch Ital Biol 146:133–146

Bridge H, Cowey A, Ragge N, Watkins K (2009) Imaging studies in congenital anophthalmia reveal preservation of brain architecture in 'visual' cortex. Brain 132:3467–3480. doi:10.1093/brain/awp279

Burgel U, Schormann T, Schleicher A, Zilles K (1999) Mapping of histologically identified long fiber tracts in human cerebral hemispheres to the MRI volume of a reference brain: position and spatial variability of the optic radiation. NeuroImage 10:489–499. doi:10.1006/nimg.1999.0497

Burgel U, Amunts K, Hoemke L, Mohlberg H, Gilsbach JM, Zilles K (2006) White matter fiber tracts of the human brain: three-dimensional mapping at microscopic resolution, topography and intersubject variability. NeuroImage 29:1092–1105. doi:10.1016/j.neuroimage.2005.08.040

Burnett LR, Stein BE, Chaponis D, Wallace MT (2004) Superior colliculus lesions preferentially disrupt multisensory orientation. Neuroscience 124:535–547. doi:10.1016/j.neuroscience.2003.12.026

Cappe C, Morel A, Barone P, Rouiller EM (2009) The thalamocortical projection systems in primate: an anatomical support for multisensory and sensorimotor interplay. Cereb Cortex 19:2025–2037. doi:10.1093/cercor/bhn228

Cattaneo Z, Vecchi T, Cornoldi C, Mammarella I, Bonino D, Ricciardi E, Pietrini P (2008) Imagery and spatial processes in blindness and visual impairment. Neurosci Biobehav Rev 32:1346–1360. doi:10.1016/j.neubiorev.2008.05.002

Chabot N, Robert S, Tremblay R, Miceli D, Boire D, Bronchti G (2007) Audition differently activates the visual system in neonatally enucleated mice compared with anophthalmic mutants. Eur J Neurosci 26:2334–2348. doi:10.1111/j.1460-9568.2007.05854.x

Chebat DR, Chen JK, Schneider F, Ptito A, Kupers R, Ptito M (2007) Alterations in right posterior hippocampus in early blind individuals. NeuroReport 18:329–333. doi:10.1097/WNR.0b013e32802b70f8

Chen Z, Wang J, Lin F, Dai H, Mu K, Zhang H (2013) Correlation between lateral geniculate nucleus atrophy and damage to the optic disc in glaucoma. J Neuroradiol 40:281–287. doi:10.1016/j.neurad.2012.10.004

Collignon O, Dormal G, Albouy G, Vandewalle G, Voss P, Phillips C, Lepore F (2013) Impact of blindness onset on the functional organization and the connectivity of the occipital cortex. Brain 136:2769–2783. doi:10.1093/brain/awt176

Crish SD, Dengler-Crish CM, Catania KC (2006) Central visual system of the naked mole-rat (*Heterocephalus glaber*). Anat Record Part A Discov Mol Cell Evol Biol 288:205–212. doi:10.1002/ar.a.20288

Cullen MJ, Kaiserman-Abramof IR (1976) Cytological organization of the dorsal lateral geniculate nuclei in mutant anophthalmic and postnatally enucleated mice. J Neurocytol 5:407–424

Dai H et al (2011) Assessment of lateral geniculate nucleus atrophy with 3T MR imaging and correlation with clinical stage of glaucoma. AJNR Am J Neuroradiol 32:1347–1353. doi:10.3174/ajnr.A2486

Desgent S, Ptito M (2012) Cortical GABAergic interneurons in cross-modal plasticity following early blindness. Neural Plasticity 2012:590725. doi:10.1155/2012/590725

DuBois RM, Cohen MS (2000) Spatiotopic organization in human superior colliculus observed with fMRI. NeuroImage 12:63–70. doi:10.1006/nimg.2000.0590

Ehrsson HH (2007) The experimental induction of out-of-body experiences. Science 317:1048. doi:10.1126/science.1142175

Eickhoff SB, Stephan KE, Mohlberg H, Grefkes C, Fink GR, Amunts K, Zilles K (2005) A new SPM toolbox for combining probabilistic cytoarchitectonic maps and functional imaging data. NeuroImage 25:1325–1335. doi:10.1016/j.neuroimage.2004.12.034

Felleman DJ, Van Essen DC (1991) Distributed hierarchical processing in the primate cerebral cortex. Cereb Cortex 1:1–47

Fonov V, Evans AC, Botteron K, Almli CR, McKinstry RC, Collins DL, Brain Development Cooperative Group (2011) Unbiased average age-appropriate atlases for pediatric studies. NeuroImage 54:313–327. doi:10.1016/j.neuroimage.2010.07.033

Fortin M et al (2008) Wayfinding in the blind: larger hippocampal volume and supranormal spatial navigation. Brain 131:2995–3005. doi:10.1093/brain/awn250

Frost DO, Boire D, Gingras G, Ptito M (2000) Surgically created neural pathways mediate visual pattern discrimination. Proc Natl Acad Sci USA 97:11068–11073. doi:10.1073/pnas.190179997

Ghazanfar AA, Schroeder CE (2006) Is neocortex essentially multisensory? Trends Cogn Sci 10:278–285. doi:10.1016/j.tics.2006.04.008

Gupta N, Greenberg G, de Tilly LN, Gray B, Polemidiotis M, Yucel YH (2009) Atrophy of the lateral geniculate nucleus in human glaucoma detected by magnetic resonance imaging. Br J Ophthalmol 93:56–60. doi:10.1136/bjo.2008.138172

Headon MP, Powell TP (1973) Cellular changes in the lateral geniculate nucleus of infant monkeys after suture of the eyelids. J Anat 116:135–145

Heil P, Bronchti G, Wollberg Z, Scheich H (1991) Invasion of visual cortex by the auditory system in the naturally blind mole rat. NeuroReport 2:735–738

Hendelman WJ (2005) Atlas of functional neuroanatomy, 2nd edn. CRC Press, Boca Raton

Hernowo AT, Boucard CC, Jansonius NM, Hooymans JM, Cornelissen FW (2011) Automated morphometry of the visual pathway in primary open-angle glaucoma. Invest Ophthalmol Vis Sci 52:2758–2766. doi:10.1167/iovs.10-5682

Heumann D, Rabinowicz T (1980) Postnatal development of the dorsal lateral geniculate nucleus in the normal and enucleated albino mouse. Exp Brain Res 38:75–85

Hilbig H, Bidmon HJ, Zilles K, Busecke K (1999) Neuronal and glial structures of the superficial layers of the human superior colliculus. Anat Embryol 200:103–115

Iglesias JE, Liu CY, Thompson PM, Tu Z (2011) Robust brain extraction across datasets and comparison with publicly available methods. IEEE Trans Med Imaging 30:1617–1634. doi:10.1109/TMI.2011.2138152

Ioannides AA, Liu L, Poghosyan V, Saridis GA, Gjedde A, Ptito M, Kupers R (2013) MEG reveals a fast pathway from somatosensory cortex to occipital areas via posterior parietal cortex in a blind subject. Front Hum Neurosci 7:429. doi:10.3389/fnhum.2013.00429

Jenkinson M, Bannister P, Brady M, Smith S (2002) Improved optimization for the robust and accurate linear registration and motion correction of brain images. NeuroImage 17:825–841

Jenkinson M, Beckmann CF, Behrens TE, Woolrich MW, Smith SM (2012) Fsl. NeuroImage 62:782–790. doi:10.1016/j.neuroimage.2011.09.015

Jiang J et al (2009) Thick visual cortex in the early blind. J Neurosci 29:2205–2211. doi:10.1523/JNEUROSCI.5451-08.2009

Johansen-Berg H, Behrens TE, Sillery E, Ciccarelli O, Thompson AJ, Smith SM, Matthews PM (2005) Functional-anatomical validation and individual variation of diffusion tractography-based segmentation of the human thalamus. Cereb Cortex 15:31–39. doi:10.1093/cercor/bhh105

Kahn DM, Krubitzer L (2002) Retinofugal projections in the short-tailed opossum (*Monodelphis domestica*). J Comp Neurol 447:114–127. doi:10.1002/cne.10206

Kang DH, Kwon KW, Gu BM, Choi JS, Jang JH, Kwon JS (2008) Structural abnormalities of the right inferior colliculus in schizophrenia. Psychiatry Res 164:160–165. doi:10.1016/j.pscychresns.2007.12.023

Karlen SJ, Krubitzer L (2009) Effects of bilateral enucleation on the size of visual and nonvisual areas of the brain. Cereb Cortex 19:1360–1371. doi:10.1093/cercor/bhn176

Karlen SJ, Kahn DM, Krubitzer L (2006) Early blindness results in abnormal corticocortical and thalamocortical connections. Neuroscience 142:843–858. doi:10.1016/j.neuroscience.2006.06.055

Katyal S, Zughni S, Greene C, Ress D (2010) Topography of covert visual attention in human superior colliculus. J Neurophysiol 104:3074–3083. doi:10.1152/jn.00283.2010

Klinge C, Eippert F, Roder B, Buchel C (2010) Corticocortical connections mediate primary visual cortex responses to auditory stimulation in the blind. J Neurosci 30:12798–12805. doi:10.1523/JNEUROSCI.2384-10.2010

Korsholm K, Madsen KH, Frederiksen JL, Skimminge A, Lund TE (2007) Recovery from optic neuritis: an ROI-based analysis of LGN and visual cortical areas. Brain 130:1244–1253. doi:10.1093/brain/awm045

Krebs RM et al (2010) High-field FMRI reveals brain activation patterns underlying saccade execution in the human superior colliculus. PLoS ONE 5:e8691. doi:10.1371/journal.pone.0008691

Kupers R, Ptito M (2011) Insights from darkness: what the study of blindness has taught us about brain structure and function. Prog Brain Res 192:17–31. doi:10.1016/B978-0-444-53355-5.00002-6

Kupers R, Ptito M (2014) Compensatory plasticity and cross-modal reorganization following early visual deprivation. Neurosci Biobehav Rev 41:36–52. doi:10.1016/j.neubiorev.2013.08.001

Kupers R, Fumal A, de Noordhout AM, Gjedde A, Schoenen J, Ptito M (2006) Transcranial magnetic stimulation of the visual cortex induces somatotopically organized qualia in blind subjects. Proc Natl Acad Sci USA 103:13256–13260. doi:10.1073/pnas.0602925103

Kupers R, Beaulieu-Lefebvre M, Schneider FC, Kassuba T, Paulson OB, Siebner HR, Ptito M (2011) Neural correlates of olfactory processing in congenital blindness. Neuropsychologia 49:2037–2044. doi:10.1016/j.neuropsychologia.2011.03.033

Lee JY et al (2014) An investigation of lateral geniculate nucleus volume in patients with primary open-angle glaucoma using 7 tesla magnetic resonance imaging. Invest Ophthalmol Vis Sci 55:3468–3476. doi:10.1167/iovs.14-13902

Leh SE, Johansen-Berg H, Ptito A (2006) Unconscious vision: new insights into the neuronal correlate of blindsight using diffusion tractography. Brain 129:1822–1832. doi:10.1093/brain/awl111

Leh SE, Ptito A, Schonwiesner M, Chakravarty MM, Mullen KT (2010) Blindsight mediated by an S-cone-independent collicular pathway: an fMRI study in hemispherectomized subjects. J Cogn Neurosci 22:670–682. doi:10.1162/jocn.2009.21217

Leo A, Bernardi G, Handjaras G, Bonino D, Ricciardi E, Pietrini P (2012) Increased BOLD variability in the parietal cortex and enhanced parieto-occipital connectivity during tactile perception in congenitally blind individuals. Neural Plasticity 2012:720278. doi:10.1155/2012/720278

Lepore N et al (2009) Pattern of hippocampal shape and volume differences in blind subjects. NeuroImage 46:949–957. doi:10.1016/j.neuroimage.2009.01.071

Lepore N et al (2010) Brain structure changes visualized in early- and late-onset blind subjects. NeuroImage 49:134–140. doi:10.1016/j.neuroimage.2009.07.048

Li M et al (2012) Quantification of the human lateral geniculate nucleus in vivo using MR imaging based on morphometry: volume loss with age. AJNR Am J Neuroradiol 33:915–921. doi:10.3174/ajnr.A2884

Limbrick-Oldfield EH, Brooks JC, Wise RJ, Padormo F, Hajnal JV, Beckmann CF, Ungless MA (2012) Identification and characterisation of midbrain nuclei using optimised functional magnetic resonance imaging. NeuroImage 59:1230–1238. doi:10.1016/j.neuroimage.2011.08.016

Liu Y et al (2007) Whole brain functional connectivity in the early blind. Brain 130:2085–2096. doi:10.1093/brain/awm121

Lund RD, Lund JS (1971) Synaptic adjustment after deafferentation of the superior colliculus of the rat. Science 171:804–807

Masucci EF, Borts FT, Perl SM, Wener L, Schwankhaus J, Kurtzke JF (1995) MR vs CT in progressive supranuclear palsy Computerized medical imaging and graphics : the official journal of the Computerized Medical Imaging Society 19:361–368

May PJ (2006) The mammalian superior colliculus: laminar structure and connections. Prog Brain Res 151:321–378. doi:10.1016/S0079-6123(05)51011-2

Merabet LB, Pascual-Leone A (2010) Neural reorganization following sensory loss: the opportunity of change. Nat Rev Neurosci 11:44–52. doi:10.1038/nrn2758

Naidich TP, Duvernoy HM, Delman BN, Sorensen AG, Kollias SS, Haacke EM (2009) Duvernoy's atlas of the human brain stem and cerebellum. Springer, Wien

Nichols TE, Holmes AP (2002) Nonparametric permutation tests for functional neuroimaging: a primer with examples. Hum Brain Mapp 15:1–25

Noppeney U (2007) The effects of visual deprivation on functional and structural organization of the human brain. Neurosci Biobehav Rev 31:1169–1180. doi:10.1016/j.neubiorev.2007.04.012

Noppeney U, Friston KJ, Ashburner J, Frackowiak R, Price CJ (2005) Early visual deprivation induces structural plasticity in gray and white matter. Curr Biol 15:R488–490. doi:10.1016/j.cub.2005.06.053

Pan WJ, Wu G, Li CX, Lin F, Sun J, Lei H (2007) Progressive atrophy in the optic pathway and visual cortex of early blind Chinese adults: a voxel-based morphometry magnetic resonance imaging study. NeuroImage 37:212–220. doi:10.1016/j.neuroimage.2007.05.014

Park HJ, Lee JD, Kim EY, Park B, Oh MK, Lee S, Kim JJ (2009) Morphological alterations in the congenital blind based on the analysis of cortical thickness and surface area. NeuroImage 47:98–106. doi:10.1016/j.neuroimage.2009.03.076

Patenaude B, Smith SM, Kennedy DN, Jenkinson M (2011) A Bayesian model of shape and appearance for subcortical brain segmentation. NeuroImage 56:907–922. doi:10.1016/j.neuroimage.2011.02.046

Pavani F, Spence C, Driver J (2000) Visual capture of touch: out-of-the-body experiences with rubber gloves. Psychol Sci 11:353–359

Pietrini P et al (2004) Beyond sensory images: object-based representation in the human ventral pathway. Proc Natl Acad Sci USA 101:5658–5663. doi:10.1073/pnas.0400707101

Ptito M, Desgent S (2006) Sensory Input-Based Adaptation and Brain Architecture. In: Baltes PB, Reuter-Lorenz PA, Rosler F (eds) Lifespan development and the brain. Cambridge University Press, Cambridge, pp 111–133

Ptito M, Kupers R (2005) Cross-modal plasticity in early blindness. J Integr Neurosci 4:479–488

Ptito M, Moesgaard SM, Gjedde A, Kupers R (2005) Cross-modal plasticity revealed by electrotactile stimulation of the tongue in the congenitally blind. Brain 128:606–614. doi:10.1093/brain/awh380

Ptito M, Schneider FC, Paulson OB, Kupers R (2008) Alterations of the visual pathways in congenital blindness. Exp Brain Res 187:41–49. doi:10.1007/s00221-008-1273-4

Qin W, Xuan Y, Liu Y, Jiang T, Yu C (2014) Functional connectivity density in congenitally and late blind subjects. Cereb Cortex. doi:10.1093/cercor/bhu051

Rademacher J, Burgel U, Zilles K (2002) Stereotaxic localization, intersubject variability, and interhemispheric differences of the human auditory thalamocortical system. NeuroImage 17:142–160

Rhoades RW (1980) Effects of neonatal enucleation on the functional organization of the superior colliculus in the golden hamster. J Physiol 301:383–399

Ricciardi E, Pietrini P (2011) New light from the dark: what blindness can teach us about brain function. Curr Opin Neurol 24:357–363. doi:10.1097/WCO.0b013e328348bdbf

Ricciardi E et al (2007) The effect of visual experience on the development of functional architecture in hMT+. Cereb Cortex 17:2933–2939. doi:10.1093/cercor/bhm018

Ricciardi E et al (2009) Do we really need vision? How blind people "see" the actions of others. J Neurosci 29:9719–9724. doi:10.1523/JNEUROSCI.0274-09.2009

Ricciardi E, Handjaras G, Bonino D, Vecchi T, Fadiga L, Pietrini P (2013) Beyond motor scheme: a supramodal distributed representation in the action-observation network. PLoS ONE 8:e58632. doi:10.1371/journal.pone.0058632

Ricciardi E, Bonino D, Pellegrini S, Pietrini P (2014) Mind the blind brain to understand the sighted one! Is there a supramodal cortical functional architecture? Neurosci Biobehav Rev 41:64–77. doi:10.1016/j.neubiorev.2013.10.006

Sabanciogullari V, Salk I, Balaban H, Oztoprak I, Kelkit S, Cimen M (2013) Magnetic resonance imaging mesencephalic tectum dimensions according to age and gender. Neurosciences 18:33–39

Sakakura H, Iwama K (1967) Effects of bilateral eye enucleation upon single unit activity of the lateral geniculate body in free behaving cats. Brain Res 6:667–678

Schiller PH (1977) The effect of superior colliculus ablation on saccades elicted by cortical stimulation. Brain Res 122:154–156

Schmid B, Schindelin J, Cardona A, Longair M, Heisenberg M (2010) A high-level 3D visualization API for Java and ImageJ. BMC Bioinform 11:274. doi:10.1186/1471-2105-11-274

Schneider KA, Kastner S (2009) Effects of sustained spatial attention in the human lateral geniculate nucleus and superior colliculus. J Neurosci 29:1784–1795. doi:10.1523/JNEUROSCI.4452-08.2009

Sharma J, Angelucci A, Sur M (2000) Induction of visual orientation modules in auditory cortex. Nature 404:841–847. doi:10.1038/35009043

Sherman JL, Citrin CM, Barkovich AJ, Bowen BJ (1987) MR imaging of the mesencephalic tectum: normal and pathologic variations. AJNR Am J Neuroradiol 8:59–64

Shimony JS, Burton H, Epstein AA, McLaren DG, Sun SW, Snyder AZ (2006) Diffusion tensor imaging reveals white matter reorganization in early blind humans. Cereb Cortex 16:1653–1661. doi:10.1093/cercor/bhj102

Shu N, Liu Y, Li J, Li Y, Yu C, Jiang T (2009) Altered anatomical network in early blindness revealed by diffusion tensor tractography. PLoS ONE 4:e7228. doi:10.1371/journal.pone.0007228

Smith SA, Bedi KS (1997) Unilateral eye enucleation in adult rats causes neuronal loss in the contralateral superior colliculus. J Anat 190(Pt 4):481–490

Smith SM, Nichols TE (2009) Threshold-free cluster enhancement: addressing problems of smoothing, threshold dependence and localisation in cluster inference. NeuroImage 44:83–98. doi:10.1016/j.neuroimage.2008.03.061

Smith SM et al (2004) Advances in functional and structural MR image analysis and implementation as FSL. NeuroImage 23(Suppl 1):S208–219. doi:10.1016/j.neuroimage.2004.07.051

Sparks DL, Hartwich-Young R (1989) The deep layers of the superior colliculus. Rev Oculomot Res 3:213–255

Sur M, Garraghty PE, Roe AW (1988) Experimentally induced visual projections into auditory thalamus and cortex. Science 242:1437–1441

Sylvester R, Josephs O, Driver J, Rees G (2007) Visual FMRI responses in human superior colliculus show a temporal-nasal asymmetry that is absent in lateral geniculate and visual cortex. J Neurophysiol 97:1495–1502. doi:10.1152/jn.00835.2006

Theoret H, Boire D, Herbin M, Ptito M (2001) Anatomical sparing in the superior colliculus of hemispherectomized monkeys. Brain Res 894:274–280

Tiao YC, Blakemore C (1976) Functional organization in the superior colliculus of the golden hamster. J Comp Neurol 168:483–503. doi:10.1002/cne.901680404

Tomaiuolo F et al (2014) Morphometric changes of the corpus callosum in congenital blindness. PLoS ONE 9:e107871. doi:10.1371/journal.pone.0107871

Trampel R, Ott DV, Turner R (2011) Do the congenitally blind have a stria of Gennari? First intracortical insights in vivo. Cereb Cortex 21:2075–2081. doi:10.1093/cercor/bhq282

Van Essen DC, Drury HA, Dickson J, Harwell J, Hanlon D, Anderson CH (2001) An integrated software suite for surface-based analyses of cerebral cortex. J Am Med Inf Assoc JAMIA 8:443–459

von Melchner L, Pallas SL, Sur M (2000) Visual behaviour mediated by retinal projections directed to the auditory pathway. Nature 404:871–876. doi:10.1038/35009102

Wallace MT, Stein BE (1994) Cross-modal synthesis in the midbrain depends on input from cortex. J Neurophysiol 71:429–432

Wallace MT, Wilkinson LK, Stein BE (1996) Representation and integration of multiple sensory inputs in primate superior colliculus. J Neurophysiol 76:1246–1266

Wang D, Qin W, Liu Y, Zhang Y, Jiang T, Yu C (2014) Altered resting-state network connectivity in congenital blind. Hum Brain Mapp 35:2573–2581. doi:10.1002/hbm.22350

Warmuth-Metz M, Naumann M, Csoti I, Solymosi L (2001) Measurement of the midbrain diameter on routine magnetic resonance imaging: a simple and accurate method of differentiating between Parkinson disease and progressive supranuclear palsy. Arch Neurol 58:1076–1079

White BJ, Munoz DP (2011) The superior colliculus. In: Liversedge S, Gilchrist I, Everling S (eds) Oxford handbook of eye movements, 1st edn. Oxford University Press, New York, pp 195–213

Winer JA (1984) The human medial geniculate body. Hear Res 15:225–247

Winkler AM et al (2012) Measuring and comparing brain cortical surface area and other areal quantities. NeuroImage 61:1428–1443. doi:10.1016/j.neuroimage.2012.03.026

Yu C, Shu N, Li J, Qin W, Jiang T, Li K (2007) Plasticity of the corticospinal tract in early blindness revealed by quantitative analysis of fractional anisotropy based on diffusion tensor tractography. NeuroImage 36:411–417. doi:10.1016/j.neuroimage.2007.03.003

Zhang Y, Brady M, Smith S (2001) Segmentation of brain MR images through a hidden Markov random field model and the expectation-maximization algorithm. IEEE Trans Med Imaging 20:45–57. doi:10.1109/42.906424

Zhang D, Snyder AZ, Fox MD, Sansbury MW, Shimony JS, Raichle ME (2008) Intrinsic functional relations between human cerebral cortex and thalamus. J Neurophysiol 100:1740–1748. doi:10.1152/jn.90463.2008

Zvorykin VP (1980) New data on individual quantitative features of the human lateral geniculate body. Arkhiv anatomii gistologii i embriologii 78:24–27